JOURNAL OF MATERIALS SCIENCE 8 (1973) 123–135

Review: Sputtering mechanisms for amorphous and polycrystalline solids

I. S. T. TSONG, D. J. BARBER
Department of Physics, University of Essex, Colchester, UK

In this article the latest developments in the theory of sputtering of amorphous and polycrystalline targets are reviewed and comparison is made with available experimental data. Special attention is given to differences in the various theoretical approaches to the sputtering yield problem and the conclusions derived therefrom.

1. Introduction

The phenomenon of atomic ejection from solid surfaces under bombardment by energetic ions is known as "sputtering". The sputtering yield, S, is defined as the number of target atoms ejected per incoming ion. For some time, the sputtering process was thought of as an evaporation process which implied that sputtering was due to very high local temperatures created at or very near the surface by the bombarding ions. Later, however, measurements of the dependence of sputtering yield on the angle of incidence of the bombarding ions established that sputtering is really a momentum transfer process rather than an evaporation process. In the past decade various successful theories have been developed based on the model of atomic collision cascades generated inside the solid target by the bombarding ion. An incoming ion penetrates the surface and strikes a target atom. This atom is usually not itself sputtered, (at least in the case of perpendicular incidence, a struck atom always has a velocity component in the direction away from the target surface), but in its turn, collides with neighbouring lattice atoms producing secondary displacements. Some of these recoil atoms have the possibility of getting scattered back towards the surface with sufficient energy to collide with and liberate surface atoms. Meanwhile, the incident ion describes a random path within the solid, losing energy by nuclear collisions and electronic excitation and finally either comes to rest or leaves the surface as a sputtered atom. Thus sputtering is a typical multiple collision process involving a cascade of moving target atoms.

In the present article we shall consider only the sputtering of amorphous and polycrystalline solids. By confining ourselves to random targets we avoid other processes such as channelling, focused collisions and anisotropy of sputtering yield which are generally associated with the regular lattice structure of single crystals. In a polycrystal where any anisotropy of the ejection pattern which could be caused by regular lattice structure is small, we can assume these lattice effects can be averaged out and therefore can be treated the same way as amorphous materials. We shall review the more recent and more important theories on sputtering and make comparison with experimental data wherever possible. Generally speaking, the sputtering yield of amorphous solids is calculated under the assumption of random slowing down in an infinite medium. The steps taken are as follows: (1) to determine the energy loss in the collisions; (2) to determine the number of primary and secondary recoil atoms; (3) to find how many of these atoms arrive at the target surface; and (4) to find the atoms which have sufficient energies to overcome surface binding and appear as sputtered atoms outside the solid. In addition to consideration of the sputtering yield, we shall also discuss the sputtering efficiency of amorphous materials, γ, defined as the fraction of bombarding ion energy leaving the target surface via sputtering.

2. Sputtering yield theory

There are three recent important theories on the sputtering of amorphous and polycrystalline solids, all of which have been successful to some extent in explaining experimental observations. They are due to Thompson [1], Sigmund [2] and

Brandt and Laubert [3]. We shall endeavour to reproduce these three theories here in a condensed form so that we can compare their different approach to the sputtering yield problem. In doing so, we try to adhere as closely as possible to the symbols used by the respective authors so that readers can easily refer to their original papers if necessary.

2.1. Thompson's theory (1968)

Consider an interaction between a bombarding particle and an infinite solid, leading to atoms recoiling from their lattice sites with energy E_2. This is called the primary event.

The density of atoms recoiling in the energy range between E_2 and $E_2 + \mathrm{d}E_2$

$$= q(E_2)\,\mathrm{d}E_2\,. \tag{1}$$

Each of the primary recoils generates a secondary collision cascade in which energy is shared by a series of two-body collisions. For one recoil at E_2, the number of atoms slowed down through E' is given by a function $\nu(E_2, E')$.

Density of atoms slowed down through E' in 1 sec

$$= \int_{E'}^{\infty} q(E_2)\,\nu(E_2, E')\,\mathrm{d}E_2\,. \tag{2}$$

We can write the flux of atoms in the energy range between E' and $E' + \mathrm{d}E'$ crossing any internal surface and travelling into a solid angle $\mathrm{d}\Omega'$ in direction $\mathbf{r}'$ as:

$$\Phi'(E', \mathbf{r}')\,\mathrm{d}E'\,\mathrm{d}\Omega' = \int_{E'}^{\infty} \frac{q(E_2)\,\nu(E_2, E')}{\mathrm{d}E'/\mathrm{d}x}\,\mathrm{d}E_2\,\frac{\cos\theta\,\mathrm{d}\Omega'\,\mathrm{d}E'}{4\pi} \tag{3}$$

where $\mathrm{d}E'/\mathrm{d}x$ is the energy loss per unit path length of the atoms in the secondary cascades.

It can be shown [4] that for a random cascade

$$\nu(E_2, E') = \eta E_2/E' \tag{4}$$

where η is of order unity and is equal to 0.52 assuming an inverse square form of potential between colliding atoms.

For the term $\mathrm{d}E'/\mathrm{d}x$ we neglect energy loss due to electronic excitation (true for ion energy below $\sim M_2$ keV [5]), and consider only energy transfers in elastic collisions between target atoms (mass M_2). Then

$$\mathrm{d}E'/\mathrm{d}x \simeq E'/D \tag{5}$$

where D is the nearest neighbouring spacing.

Substituting Equations 4 and 5 into Equation 3, we obtain

$$\Phi'(E', \mathbf{r}')\,\mathrm{d}E'\,\mathrm{d}\Omega' = \frac{\eta D}{E'^2}\int_{E'}^{\infty} q(E_2)\,E_2\,\mathrm{d}E_2\,\frac{\cos\theta\,\mathrm{d}\Omega'\,\mathrm{d}E'}{4\pi} \tag{6}$$

provided E' is small compared to E_2 and can be brought out of the integral.

Now we have to find $q(E_2)$, the function which determines the density of recoil atoms. Let us assume the incident ion has mass M_1 and energy E_1 and target atoms mass M_2 and energy E_2. Their interaction is characterized by the Screened Coulomb potential, sometimes called Thomas-Fermi potential,

$$V(r) = \frac{Z_1 Z_2\,\epsilon^2}{r}\exp(-r/a) \tag{7}$$

where $a = Ca_0/(Z_1 Z_2)^{1/6}$, C is a constant of the order unity and ϵ is the electronic charge. For a limited range of r, one can fit an inverse square function to the screened Coulomb potential [5] and obtain

$$V(r) = \frac{2E_{\mathrm{R}}}{e}(Z_1 Z_2)^{5/6}(a_0/r)^2 \tag{8}$$

where $E_{\mathrm{R}} = \epsilon^2/2a_0 = 13.6$ eV; $a_0 = 0.53$Å and $e = 2.718$.

Equation 8 is applicable to ion energy range from 10^3 to 10^5 eV. For lower energies the Born-Mayer potential

$$V(r) = A\exp(-r/b)$$

has to be used.

From $V(r)$ one can calculate $\mathrm{d}\sigma/\mathrm{d}E_2$, the differential cross section for producing a primary event [5], and using the fact that

$$q(E_2) = n\Phi_1\,.\,\mathrm{d}\sigma/\mathrm{d}E_2$$

where n = density of target atoms, Φ_1 = flux of bombarding ion crossing unit area normal to their path, we find:

$$q(E_2) = \frac{\pi^2 a^2 n E_{\mathrm{a}} \Lambda^{\frac{1}{2}}\Phi_1}{8E_1^{\frac{1}{2}}E_2^{3/2}} \quad \text{for } E_2 < \Lambda E_1 \tag{9}$$

where ΛE_1 = maximum recoil energy = $\frac{4M_1M_2}{(M_1+M_2)^2}E_1$; a = screening radius = $a_0/(Z_1Z_2)^{1/6}$; E_{a} = the value of E_1 which gives the distance of closest approach a, in a head-on collision = $2E_{\mathrm{R}}(Z_1Z_2)^{7/6}(M_1+M_2)/eM_2$.

To transform $\Phi'(E')$, the flux inside the solid.

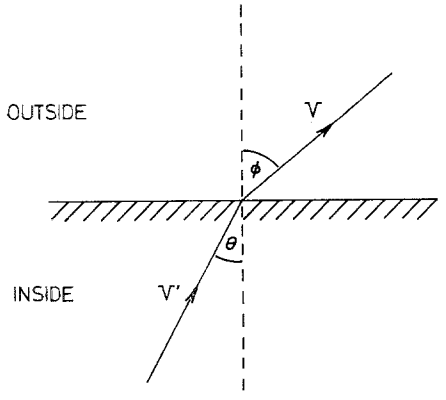

Figure 1 Change in magnitude and direction of the velocity of an atom leaving a target surface.

into $\Phi(E)$, the flux which can be measured outside the surface, a simple assumption is made of a binding force normal to the surface. So when an atom leaves the surface, its velocity component parallel to the surface will be unaffected but the normal component of its kinetic energy will be reduced by E_b.

This means that parallel to the surface (see Fig. 1), we have

$$v' \sin'\theta = v \sin\phi$$

and normal to the surface

$$E' = E + E_b .$$

From these two equations we can transform Equation 6 into:

$$\Phi(E, \phi)\, \mathrm{d}\Omega\, \mathrm{d}E = \frac{\eta D \cos\phi}{4\pi(1 + E_b/E)^3 E^2} \int_{E+E_b}^{\infty} E_2\, q(E_2)\, \mathrm{d}E_2\, \mathrm{d}\Omega\, \mathrm{d}E . \quad (10)$$

If we consider the spectrum as a function of E at a fixed angle ϕ, then at energies where $E_b \ll E \ll E_2$, we see that approximately

$$\Phi(E) \propto 1/E^2.$$

Thompson [1] has shown experimentally that the energy spectra of ejected Au atoms under bombardment by Ar^+ and Xe^+ ions exhibit this E^{-2} dependence, and indeed the main purpose of Thompson's theory was to predict the shape of the energy spectrum.

Now if we substitute Equation 9 into Equation 10 and integrate first over $\mathrm{d}\Omega$ with Φ going from 0 to $\pi/2$ and then over $\mathrm{d}E$ with E from 0 to ΛE_1 and finally divide throughout by $\Phi_1 \cos\psi$ where ψ is the angle of ion incidence, we obtain the sputtering yield in atoms/ion:

$$S = \frac{\pi^2 a_0^2 n^{2/3}}{8e} \frac{E_R}{E_b} \frac{M_1 (Z_1 Z_2)^{5/6}}{M_1 + M_2} \sec\psi \quad (11)$$

where we have put $D = n^{-1/3}$ and $\eta = \frac{1}{2}$.

The important points in this expression are that: (1) S is proportional to a function of the atomic masses and atomic numbers of the bombarding ion and target atom; (2) S is independent of E_1, the energy of the bombarding ions in the range $E_b \ll E_1 \leqslant E_a$. E_b = sublimation energy $\simeq$ 3 to 5 eV for metals, $E_a \simeq 1$ to 100 keV; (3) S is proportional to $\sec\psi$.

2.2. Sigmund's theory (1969)

The target surface under bombardment is assumed to have a planar surface. Consider a collision cascade initiated by an ion which starts its motion in a plane $x = 0$ at a time $t = 0$. The distribution function

$$G(x, \mathbf{v}_0, \mathbf{v}, t)\, \mathrm{d}^3 v_0\, \mathrm{d}x \quad (12)$$

defines the number of atoms which, at time t, are moving in a layer between x and $x + \mathrm{d}x$ and have velocities lying within a velocity-space element $\mathrm{d}^3 v_0$ about $\mathbf{v}_0$.

The sputtering yield for backward sputtering of a target with a plane surface at $x = 0$ can be written as

$$S = \int \mathrm{d}^3 v_0 |v_{0x}| \int_0^{\infty} \mathrm{d}t\, G(0, v_0, \mathbf{v}, t) \quad (13)$$

where

$$\frac{\mathrm{d}x}{\mathrm{d}t} = v_{0x} .$$

Now we write

$$F(x, \mathbf{v}_0, \mathbf{v}) = \int_0^{\infty} G(x, \mathbf{v}_0, \mathbf{v})\, \mathrm{d}t \quad (14)$$

$F(x, \mathbf{v}_0, \mathbf{v})|v_{0x}|\mathrm{d}^3 v_0$ is the total number of atoms that penetrate the plane x with a velocity $(\mathbf{v}_0, \mathrm{d}^3 v_0)$ during the period of the collision cascade.

We then introduce the function

$$H(x, \mathbf{v}) = \int \mathrm{d}^3 v_0 |v_{0x}| F(x, \mathbf{v}_0, \mathbf{v}) \quad (15)$$

which in fact represents the sputtering yield for the case where the starting point of the cascade is at $x = 0$ and the sputtered surface is in the plane x. Thus $H(x, \mathbf{v})$ is measurable in principle for $x \leqslant 0$ for backward sputtering.

Next we replace velocity variables with energy variables and write the sputtering yield as

$$S(E, \eta) = H(x = 0, E, \eta) \qquad (16)$$

where E = energy of the impinging particle and η = direction cosine relative to x-axis.

Finally, the Boltzmann transport equation is formulated in terms of $H(x, E, \eta)$ and solved using the Legendre polynomial expansion

$$H(x, E, \eta) = \sum_{l=0}^{\infty} (2l + 1)\, H_l(x, E)\, P_l(\eta) \qquad (17)$$

where $P_l(\eta)$ are Legendre polynomials.

To solve the Boltzmann equation, other input quantities such as electronic stopping cross section, the differential cross section for elastic collisions and the surface binding force have to be specified.

(a) For electronic stopping power, Lindhard's expression is used:

$$S_e(E) = KE^{\frac{1}{2}} . \qquad (18)$$

The constant K depends on the atomic numbers and masses of the ion and target.

(b) For the collision cross section, the power potential approximation to the Thomas-Fermi cross section for elastic scattering described by Lindhard *et al* [7, 8] is chosen. So we have:

$$d\sigma = CE^{-m}\, T^{-1-m}\, dT \qquad (19)$$

where E = projectile energy; T = recoil energy; $m = 1$ for Rutherford scattering ($= \frac{1}{2}$ for energy from 10^3 to 10^5 eV (corresponds to the case of an inverse square potential), $= \frac{1}{3}$ for energy from 10^2 to 10^3 eV, $= 0$ for energy less than 10^2 eV).

These values of m hold true for interaction between ions and atoms of medium massses.

The constant C is given by [8]:

$$C = \tfrac{1}{2}\pi\lambda_m\, a_{22}{}^2(2Z_2{}^2\, e^2/a_{22})^{2m} \qquad (20)$$

for ion and atom with equal masses

$$C = \tfrac{1}{2}\pi\, \lambda_m\, a_{12}{}^2(M_1/M_2)^m\, (2Z_1\, Z_2\, e^2/a_{12})^{2m} \qquad (21)$$

for ion and atom with unequal masses, where Z_1 and Z_2 are atomic numbers, a_{12} and a_{22} are Thomas-Fermi screening radii, and λ_m are dimensionless constants equal to

$$\lambda_1 = 0.5,\ \lambda_{\frac{1}{2}} = 0.327,\ \lambda_{1/3} = 1.309 . \qquad (22)$$

For collisions in the eV range, $m = 0$ and we have, from Equation 19:

$$d\sigma = C_0\, T^{-1}\, dT \qquad (23)$$

where

$$C_0 = \tfrac{1}{2}\pi\, \lambda_0\, a^2 \qquad (24)$$

and $\lambda_0 = 24$, $a = 0.219$Å.

The stopping power for elastic collisions is given by:

$$S_n(E) = \int_0^E T\, d\sigma = \frac{1}{1 - m}\, CE^{1-2m}. \qquad (25)$$

(c) The surface binding force which affects the ejection of a surface atom is chosen to be that of a spherically symmetric potential barrier type, i.e.

$$U(\eta_0) = U_0 \qquad (26)$$

U_0 is of the order of a few eV for most metals.

With these three input quantities the Boltzmann equation is solved using the Legendre polynomial expansion (Equation 17) to give the sputtering yield

$$H(x, E, \eta) = \frac{3}{4\pi^2}\, \frac{F(x, E, \eta)}{NC_0\, U_0} \qquad (27)$$

where $F(x, E, \eta)\, dx$ is the amount of energy deposited in a layer (x, dx) by an ion of energy E starting at $x = 0$ and by all the recoil atoms. N is the atomic density of the target.

We can rewrite Equation 27 in the form

$$H(x, E, \eta) = \Lambda F(x, E, \eta) \qquad (28)$$

where

$$\Lambda = \frac{3}{4\pi^2}\, \frac{1}{NC_0\, U_0} . \qquad (29)$$

In the elastic collision region where electronic stopping is unimportant, the distribution $F(x, E, \eta)$ is approximately Gaussian and can be approximated by the Edgeworth expansion [9, 10] in terms of the moments $\langle x^n \rangle$:

$$F(x, E, \eta) = \frac{\nu(E)}{\langle \triangle x^2 \rangle^{\frac{1}{2}}} \left[\psi_0(\xi) - \frac{1}{6}\Gamma_1\, \psi_3(\xi) - \ldots \right] \qquad (30)$$

where $\nu(E)$ is the amount of energy deposited in the target in the form of atom motion.

$$\langle \triangle x^n \rangle = \langle (x - \langle x \rangle)^n \rangle \qquad n = 2, 3, \ldots$$

$$\psi_n(\xi) = (d^n/d\xi^n)\, (2\pi)^{-\frac{1}{2}} \exp(-\xi^2/2) \qquad n = 0, 1, 2, \ldots$$

$$\xi = (x - \langle x \rangle)/\langle \triangle x^2 \rangle^{\frac{1}{2}}$$

$$\Gamma_1 = \langle \triangle x^3 \rangle / \langle \triangle x^2 \rangle^{3/2}$$

For backward sputtering at a surface at $x = 0$, we can obtain Equations 28 and 30 to give the sputtering yield

$$S(E, \eta) = \frac{\Lambda E}{\langle \triangle x^2 \rangle^{\frac{1}{2}}} \left[\psi_0(\xi_0) - \tfrac{1}{6}\Gamma_1 \psi_3(\xi_0) - \ldots\right] \quad \ldots\ldots (31)$$

where $\nu(E) = E$ in the elastic collision region and $\xi_0 = -\langle x \rangle / \langle \triangle x^2 \rangle^{\frac{1}{2}}$.

For the power cross section (Equation 19), the moments $\langle x^n \rangle$ have the general form [11]:

$$\langle x^n \rangle = (E^{2m}/NC)^n \, h_n(\eta) \qquad (32)$$

where $h_n(\eta)$ is some function of η. This means that ξ_0 and the contents of the square brackets in Equation 31 are independent of ion energy. The factor in front of the brackets is proportional to NCE^{1-2m}, which is essentially the stopping power (Equation 25). Hence the sputtering yield is a product of the stopping power and some function of the angle of ion incidence which may depend on m and the mass ratio M_2/M_1.

We note that for medium mass ions and atoms, in the energy range from 10^3 to 10^5 eV, $m = \frac{1}{2}$, which makes the sputtering yield $S(E, \eta)$ independent of ion energy. This finding agrees with that of Thompson (Equation 11).

The angular dependence of the sputtering yield is given by Sigmund as

$$\frac{S(E, \eta)}{S(E, 1)} = \eta^{-f} = (\cos \theta)^{-f} \qquad (33)$$

for not-too-oblique incidence, where $S(E, 1)$ is the yield for perpendicular incidence, $f \simeq 5/3$ for mass ratios $M_2/M_1 \lesssim 3$ and Sigmund also shows that f is nearly the same for $m = \frac{1}{2}$ and $m = \frac{1}{3}$, indicating in the energy range from 10^2 to 10^5 eV the angular variation of the yield is not sensitive to ion energy.

2.3. Theory by Brandt and Laubert (1967)

This theory is based on the concepts advanced by Lindhard *et al* [6, 7] on the energy loss by an ion travelling in a solid. A comprehensive sputtering yield curve is derived which is valid for a wide range of ion-target combinations and for all ion energies large compared with the energy required to displace a lattice atom.

Consider an incoming ion of atomic number Z_1, mass M_1 and initial energy E_1 colliding with a random target whose atoms have atomic number Z_2, mass M_2 and average density N_2. The ion loses energy by nuclear collisions and electronic excitation. After it has travelled a distance **r**, it displaces an atom from its lattice position and this atom recoils with energy E_2. This primary recoil atom creates a secondary cascade of displaced atoms. On average $\mathrm{d}n_2(E)$ secondary recoil atoms are created in the energy range between E and $E + \mathrm{d}E$.

Integrating over the whole distance travelled by the incoming ion, we can write the total number of atoms escaping from the target surface due to the atom motion caused by this ion, i.e. the sputtering yield, as

$$S = \gamma N_2 \int_{E_1} \mathrm{d}q_{12}(E_2) \int_{E_2} \mathrm{d}n_2(E) \, l_2(E_2 - E) \qquad (34)$$

where $\gamma = (\cos \theta)^{-1}$ and θ is the angle between the direction of the ion beam and the normal to the target surface; $q_{12}(E_2)$ = cross section for energy transfer between the ion and target atom; and $l_2(E_2 - E)$ = the path length of the cascade, i.e. the distance away from the site of the initial event where $dn_2(E)$ atoms are dislodged. If the ion energy is large, then we have:

$$\frac{\mathrm{d}n_2(E)}{\mathrm{d}E} = \frac{1}{U_2}(1 - d_k(E)) \qquad (35)$$

where U_2 = energy required to displace an atom from its rest position (about 20 to 30 eV for metals) and $d_k(E)$ = a numerical factor which accounts for the energy lost to electronic excitations.

Let E_c denote the energy at which electronic stopping power becomes comparable with nuclear stopping power, i.e. at ion energies $\geqslant M_2$ keV. For $E \ll E_c$, we have:

$$d_k(E) = \frac{3}{2}\alpha(E/E_c)^{\frac{1}{2}} + \ldots \qquad (36)$$

The constant α is slightly larger than unity. The stopping cross section of the target for the bombarding ions is given by

$$S_{12}(E_1) = \int_{E_1} E \, \mathrm{d}q_{12}. \qquad (37)$$

According to Brandt and Laubert, $l_2(E)$ can be written as:

$$l_2(E) \simeq l_0[1 - \exp(-L(E)/l_0)] \qquad (38)$$

where l_0 is a constant characteristic to the target material, and $L(E)$ the path length of energy propagation in the cascade.

Putting Equations 35, 37 and 38 into Equation 34, the sputtering yield becomes:

$$S = \gamma(E_1/U_2)x^{-1}[\phi(x) - \triangle_k] \qquad (39)$$

where x is a dimensionless variable given by:

$$x \equiv E_1/\{l_0 N_2 S_{12}(E_1)\} \equiv \epsilon/\{\lambda_0 \mathcal{C}_{12} \sigma(\epsilon)\} \qquad (40)$$

in which

$$\lambda_0 = 3.25 \times 10^{-3} \quad \text{for most metals} \tag{41}$$

$$\epsilon = E_1/\epsilon_{12} \tag{42}$$

where

$$\epsilon_{12} = Z_1 Z_2 \epsilon^2 (M_1 + M_2)/(a_{12} M_2) \tag{43}$$

$$a_{12} = (9\pi^2/2^7)^{1/3} a_0 (Z_1^{2/3} + Z_2^{2/3})^{-\frac{1}{2}} \tag{44}$$

$$a_0 = \hbar^2/me^2 = \text{Bohr radius} \tag{45}$$

and

$$\mathscr{C}_{12} = \{8M_1M_2/(M_1 + M_2)^2\} Z_2^{2/3}/(Z_1^{2/3} + Z_2^{2/3}) \quad \ldots\ldots (46)$$

$$\sigma(\epsilon) = \text{the scaled nuclear stopping power} = (\mathscr{L}_{12}/\epsilon_{12}) N_2 S_{12} \tag{47}$$

where

$$\mathscr{L}_{12} = (M_1 + M_2)^2/(4\pi a_{12}^2 M_1 N_2 M_2) \tag{48}$$

$\sigma(\epsilon)$ has been calculated by Lindhard *et al* [7] for the Thomas-Fermi approximation of the scattering potential (Equation 7).

Having defined x in Equation 39, Brandt and Laubert find, using Thomas-Fermi potential [8]:

$$\varphi(x) = 1 - \{2x - 1 + \exp(-2x)\}/2x^2 \tag{49}$$

and

$$\triangle_k = \alpha(x/x_c)^{\frac{1}{2}} \psi(x) \text{ for } \epsilon \ll \epsilon_c \tag{50}$$

where

$$x_c \equiv (\epsilon_c/\epsilon)x \tag{51}$$

$$\psi(x) = \tfrac{1}{2}\{1 + (3/2x^3) [1 - x - (1 + x)\exp(-2x)]\}. \tag{52}$$

At high ion energies, we can rewrite Equations 49 and 52 as:

$$\varphi(x) = 1 - x^{-1} + (2x^2)^{-1} \tag{53}$$

$$\psi(x) = \tfrac{1}{2}[1 - (3/2x^2) + (3/2x^3)]. \tag{54}$$

If electronic stopping can be neglected, i.e. $\triangle_k = 0$ in Equation 39, Brandt and Laubert show that at high ion energies ($E_1 \gg 1$ keV) the sputtering yield can be written as:

$$S = (\gamma\epsilon_{12}/U_2)\, \mathscr{C}_{12}\, \lambda_0\, \sigma(\epsilon)\,. \tag{55}$$

This means that the sputtering yield is proportional to a function of the atomic numbers and masses of the particles, proportional to the nuclear stopping power and its angular dependence goes as sec θ. In the energy range 10^3 to 10^5 eV where the Thomas-Fermi potential can be approximated to an inverse square type (see Equations 7 and 8), Lindhard [7] shows that $\sigma(\epsilon)$ becomes independent of ion energy; hence S is independent of ion energy. These conclusions reached by Brandt and Laubert are largely similar to those of Thompson and Sigmund.

3. Comparison of experimental data of sputtering yield with theory

The sputtering yield of solids has been measured by various different methods. The simplest method is the determination of mass difference of the target before and after sputtering by weighing. Another simple way sometimes favoured is by measuring the eroded volume with interference microscopy, but this method requires a smooth and reflecting surface in order to achieve reasonable accuracy. Other novel techniques of yield measurements include one of spectroscopic detection [12] in which the intensity of the emission lines of the sputtered particles as a function of ion beam current and energy is calibrated using the weight loss method. While this technique does not appear to offer any immediate advantage over the former two, its use may be more appreciated when the different sputtering yields of the various components in an alloy or a multiphase material are required since different components can be distinguished by their characteristic emission lines [13]. It is perhaps worth mentioning here that work of this kind on multiphase materials is virtually nonexistent and it is highly desirable to carry out such studies because of its practical importance.

Sputtering yield measurements on amorphous and polycrystalline solids have been widely carried out in the past 15 years or so. To interpret the experimental results in terms of the above three theories we are interested in the sputtering yield expressed as (i) a function of the ion energy, (ii) a function of angle of ion incidence and (iii) a function of masses of the incident ion and target material. However, the sputtering yield data given in terms of the ratio of atoms/ion is misleading in the majority of investigations because the parameters of the incident ion beam were not well defined. For example, most experiments were carried out without using any mass analysing attachment. This means the ion beam probably contained energetic doubly or even triply charged ions of the species under study plus a host of other impurity ions such as H^+, H_2^+, N^+, O^+, HO^+, H_2O^+ etc, due to contamination of pump vapours and degassing of the apparatus etc [14]. This puts the energy and mass of the incident ions in doubt. If the pressure in the

apparatus is high, then the energetic ions will have the probability of colliding with the neutral gas atoms giving rise to a neutral component in the ion beam. This causes an uncertainty in the determination of the number of ions arriving at the target surface. Also, back diffusion due to high pressure near the target surface will cause redeposition of particles sputtered from the target.

In view of the uncertainties which exist, exacting experimental requirements must be satisfied for reliable sputtering yield data to be obtained. It is therefore essential to use: (1) ions of definite energy, (2) ions of definite mass and charge, (3) ions with a definite angle of incidence, (4) a low pressure in the apparatus. Much of the earlier work was not performed under well-defined experimental conditions. In the following sections, we shall only discuss work in which most of the parameters have been brought under control.

3.1. Variation of sputtering yield with ion energy

Figs. 2 and 3 show the yield of polycrystalline copper as a function of Ar^+ ion energy. The yield of amorphous targets such as fused silica, Ge and Si are shown in Figs. 4 and 5. Although Ge and Si are essentially single crystals, they can be treated as amorphous under ion bombardment at room temperatures [15, 16] due to randomization of the lattice within collision cascades. From these curves it can be seen that the sputtering yield increases rapidly in a linear

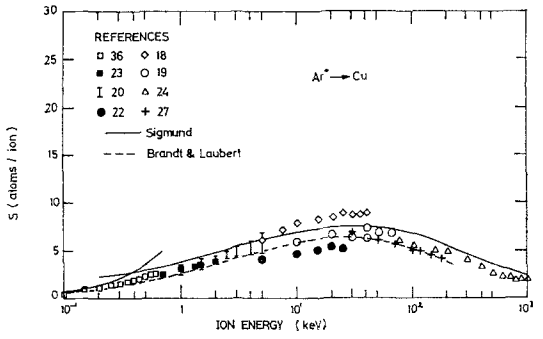

Figure 3 Comparison of theoretical sputtering yield with experimental data of Ar^+ on polycrystalline Cu at normal incidence over a wide range of ion energies.

fashion once the ion energy reaches a threshold value which is characteristic of the particular ion-target combination. Somewhere between 1 and 10 keV the curve shows a slowing-down in the rate of increase of sputtering yield, finally reaching a maximum. After this, the yield stays approximately constant in the region between 10 and 100 keV, and at higher energies the yield begins to decrease due to the ions penetrating more deeply below the target surface and very few of the atoms ejected from their lattice sites as a result of the collisions finding their way to the surface. One significant fact emerging from this curve is that the yield is virtually independent of ion energy in the range 10 to 100 keV, as predicted by all three theories. The majority of the sputtering experiments (on a variety of ion-

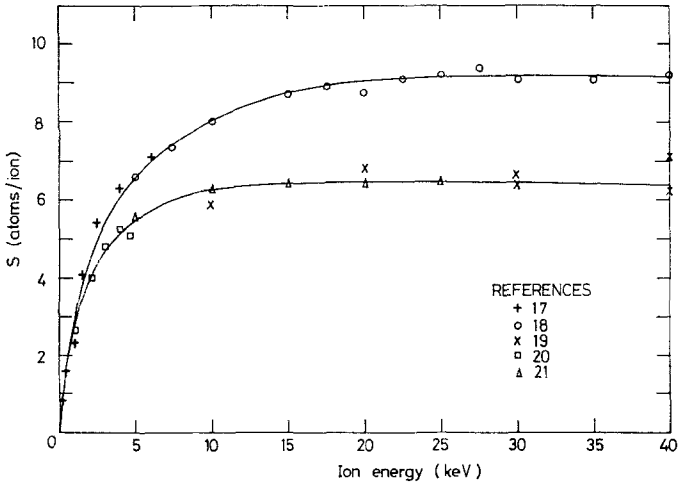

Figure 2 Variation of sputtering yield with ion energy up to 40 keV for polycrystalline Cu bombarded with Ar^+ ions at normal incidence.

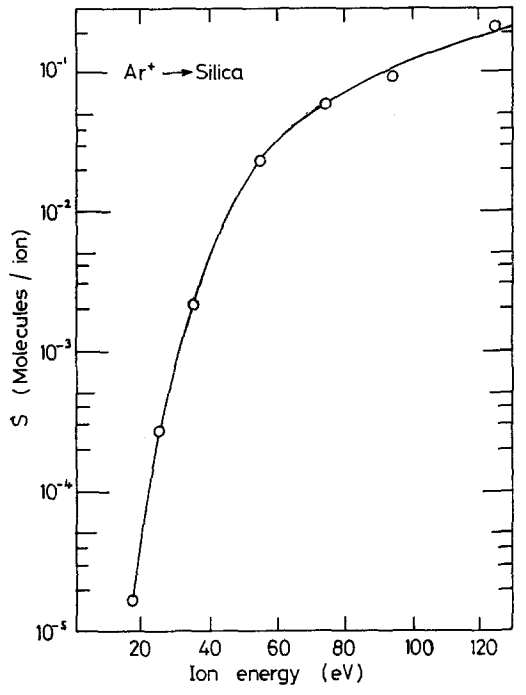

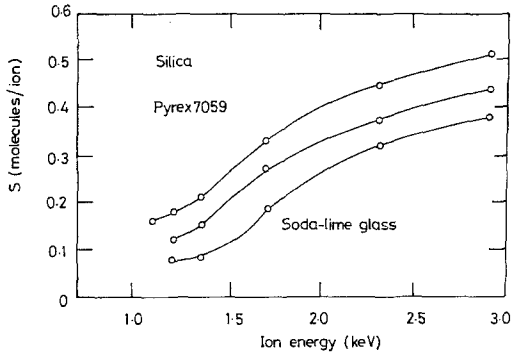

Figure 4 (a) Variation of sputtering yield with ion energy for Ar^+ on fused silica according to Jorgensen and Wehner [25]. The yield is expressed in molecules/ion despite the fact that sputtered particles mostly appear as single atoms.
Figure 4 (b) Variation of sputtering yield with ion energy on fused silica, Pyrex 7059 and soda-lime glass. Davidse and Maissel [26].

target combinations) have been carried out in this ion energy range and most of them tend to confirm the theoretical prediction of invariance. In addition, both the theory of Sigmund and that of Brandt and Laubert show reasonably good agreement over the entire range of ion energies from 0.1 to 10^3 keV.

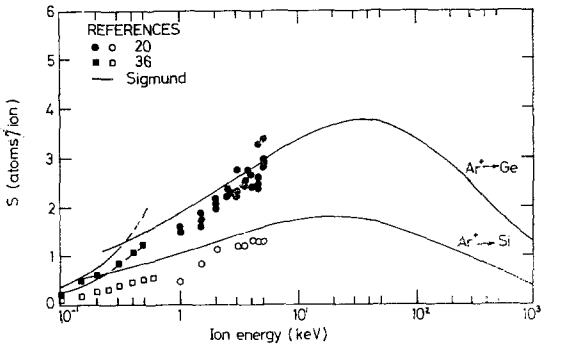

Figure 5 Sputtering yield for Ar^+ on "amorphous" targets of Si and Ge as a function of ion energy.

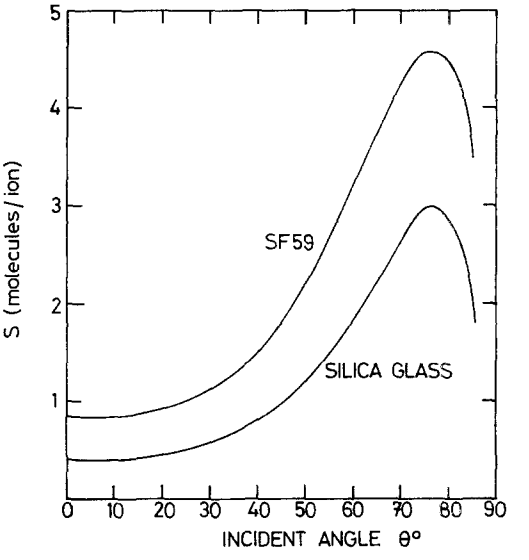

Figure 6 Variation of sputtering yield with incident angle of Ar^+ ions at 5.6 keV on Schott lead glass SF59 and silica glass. Bach [28].

3.2. Variation of sputtering yield with angle of ion incidence

Nearly all the curves of sputtering yield as a function of the angle of ion incidence display similar behaviour to that shown in Fig. 6, which describes the sputtering of silica glasses. The yield increases rather slowly in the beginning, then increases rapidly beyond about 30° (we take 0° as perpendicular incidence), finally passes through a maximum at grazing incidence and falls towards zero at $\theta = 90°$. The maximum and the falling-off can be explained by the fact that as θ increases, the incident ion has an increasing probability of being reflected without traversing

the effective surface layer because of the repulsive action of the potential barrier associated with the surface plane of atoms. Lindhard [29] shows that the critical angle for such reflection is given by:

$$\frac{\pi}{2} - \hat{\theta} = \left[\frac{5\pi\, a_0^2\, n^{2/3}\, Z_1\, Z_2\, E_R}{(Z_1^{2/3} + Z_2^{2/3})E_1}\right]^{\frac{1}{2}}. \quad (56)$$

When $\theta > \hat{\theta}$, penetration of the potential barrier is not possible. Hence $\hat{\theta}$ corresponds to the angle where the sputtering yield, S, reaches its maximum value.

In polycrystalline solids the sputtering yield can be regarded as a summation of S from all the possible orientations of individual grains and the angular dependence of S is expected to vary much the same way as that for amorphous solids shown in Fig. 6. Recently, however, Evdokimov and Molchanov [30] have observed fine structures in the sputtering curves of Kr^+, Ar^+ and Ne^+ on polycrystalline Cu and Mo thought to be due to a certain amount of close-packing at the target surface. Fig. 7 shows the variation of the yield with angle of incidence for Ar^+ ions on polycrystalline copper, together with curves calculated according to Sigmund and the sec θ relationship. Fig. 8 shows the angular dependence of the yield for self-sputtering of Nb [34].

Sigmund finds that the sec θ dependence, favoured by Thompson and Brandt and Laubert, and derived from a simple path-length consideration for an ion travelling in a solid, does not fit

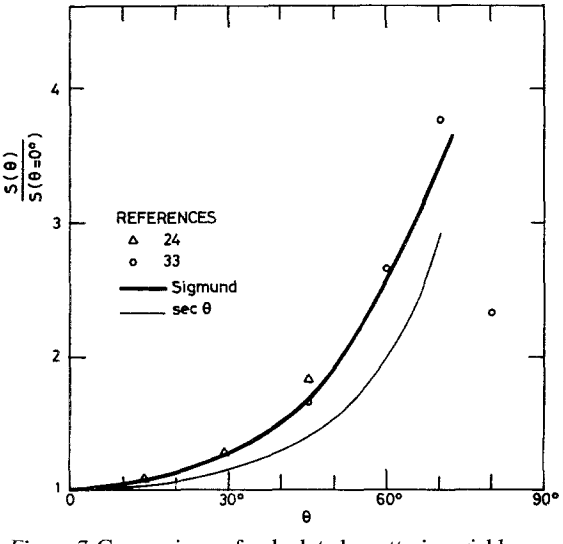

Figure 7 Comparison of calculated sputtering yield as a function of incident angle with experimental data of Ar^+ on Cu.

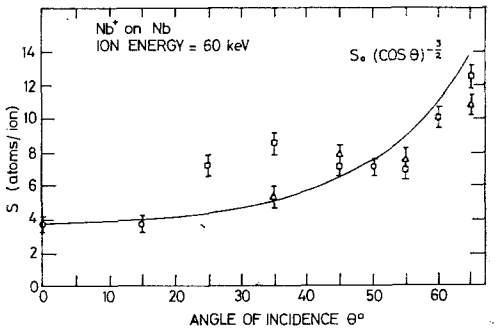

Figure 8 Variation of Nb self-sputtering yield with incident angle according to Summers *et al* [34]. Empirical relationship $S(\theta) = S(\theta = 0).(\cos\theta)^{-1.5}$ is very close to the $(\cos\theta)^{-1.6}$ dependence predicted by Sigmund.

experimental values well except for $M_1 \ll M_2$. The agreement between experimental results and Sigmund's theoretical prediction, based on calculations of the spatial distribution of the energy deposited by the bombarding ion, is generally quite good. Other forms of angular dependence of sputtering yield have been found by various workers [21, 27, 35], the details of which will not be dealt with here.

3.3. Variation of sputtering yield with the atomic numbers and masses of incident ion and tangent atom

All three theories predict complex variations of sputtering yield with the atomic numbers and masses of the incident ion and target atom. The experiments of Almen and Bruce [19] and Rol *et al* [21] appeared to confirm this. Their results are shown in Tables I and II and Fig. 9. Gener-

TABLE I Sputtering yield for Ne^+, Ar^+, Kr^+ and Xe^+ ions at 45 keV on different polycrystalline target materials. Almen and Bruce [19].

Target material	Sputtering yield (atoms/ion)			
	Ne	Ar	Kr	Xe
V	0.3	1.0	1.7	1.9
Fe	1.3	2.3	4.0	4.9
Ni	1.4	3.5	5.6	7.6
Cu	3.2	6.8	11.8	19.0
Mo	0.6	1.5	2.7	3.8
Pd	2.5	5.3	10.5	14.4
Ag	4.5	10.8	23.5	36.2
Sn	1.8	4.3	8.5	11.8
Ta	0.7	1.6	3.1	4.0
W	1.0	2.3	4.7	6.4
Pt	1.9	5.3	11.3	16.0
Au	3.6	10.2	24.5	39.0
Pb	3.6	10.5	24.0	44.5

TABLE II Sputtering yield expressed in atoms/ion for polycrystalline copper bombarded with the following ions at 15 keV. Rol *et al* [21].

Ion	N	Ne	Na	Si	P
yield	2.0	3.2	2.7	3.9	4.7
Ion	S	Cl	Ar	K	Cu
yield	3.8	5.2	6.3	5.2	6.8
Ion	Zn	Cd	I	Hg	Tl
yield	7.1	10.5	11.0	11.2	13.1

ally speaking, the sputtering yield tends to increase with increasing ion mass for the same target material, whereas the same cannot be said for increasing target mass for the same incident ion. Sigmund [2] has calculated the yield for various target materials bombarded by 400 eV Xenon ions and obtained reasonable agreement with experimental data [36]. The sputtering yield for a variety of amorphous targets bombarded by 5 keV Ar^+ ions has been measured by Bach [37] and compared with theoretical values according to Brandt and Laubert. Good agreement was obtained for SiO_2, TiO_2 and ZnS. More recently Bach [38] has reported the sputtering yield of silica glass bombarded by Ne^+, Ar^+ and Xe^+ ions and reasonable agreement between experimental and calculated values was again achieved.

Andersen and Bay [39] have performed sputtering experiments in ultrahigh vacuum conditions to measure the yield of copper bombarded by 21 different ions at 45 keV. It was found that the measured sputtering yield depended sensitively on the previous irradiation history of the target which changes the ejection conditions at the surface. This is thought to be due to volume diffusion (possibly damage-enhanced) or surface diffusion, giving rise to a

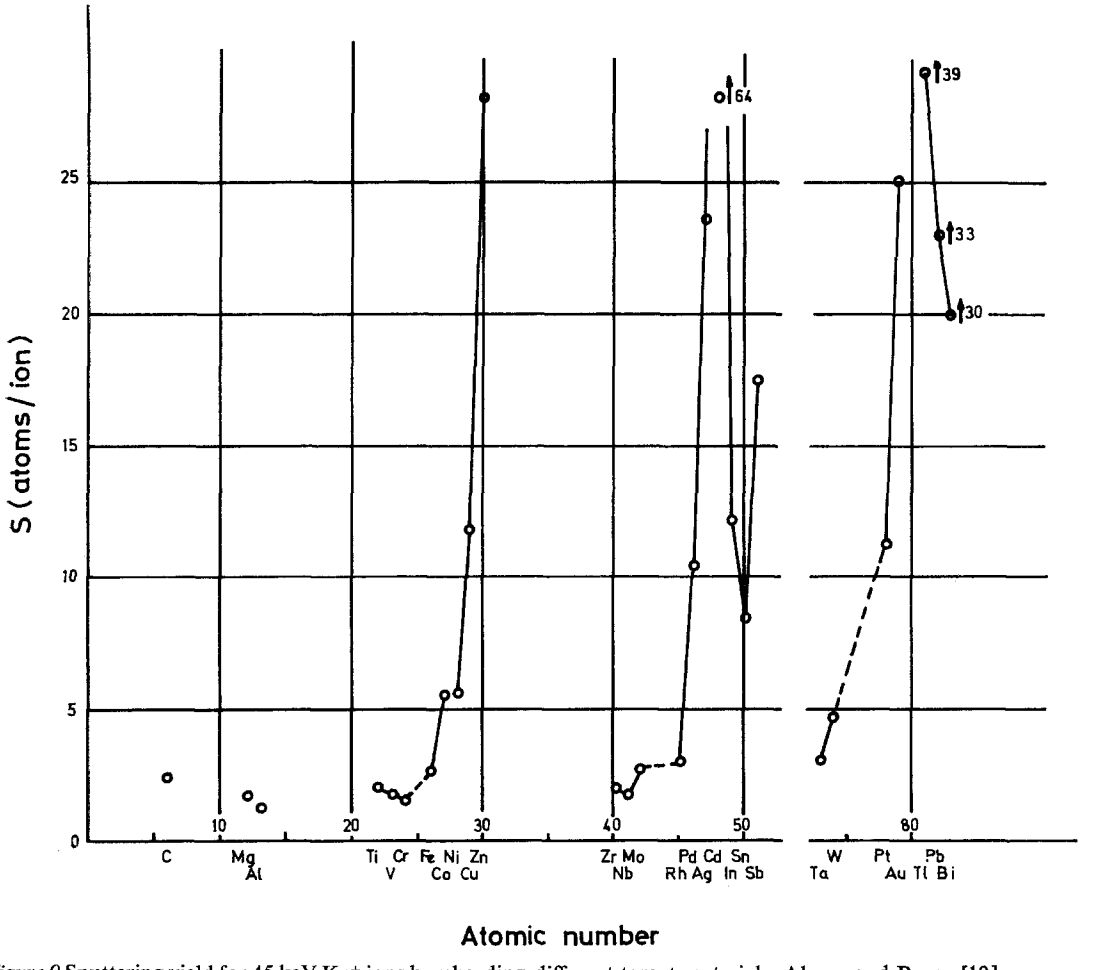

Figure 9 Sputtering yield for 45 keV Kr^+ ions bombarding different target materials. Almen and Bruce [19].

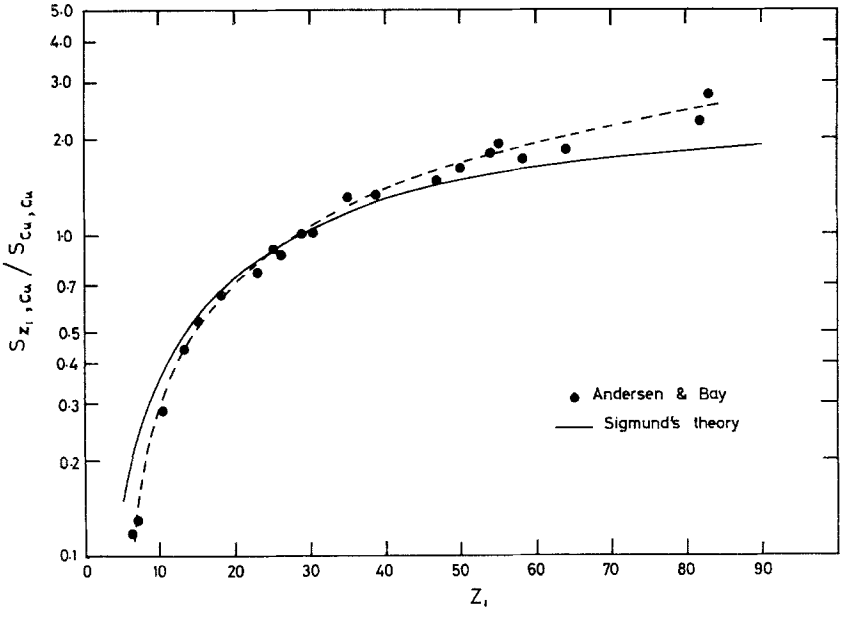

Figure 10 Sputtering yield ratio of copper for 21 different 45 keV ions together with the theoretical prediction of Sigmund.

clustering of projectile atoms with a low yield on the target surface. These effects make it difficult to define an absolute yield for many systems. The sputtering yield at perpendicular incidence from Sigmund's theory (Equation 31) can be written as

$$S = \text{Const.}\ \alpha\ S_n(Z_1, Z_2)/U_0 \qquad (57)$$

where $S_n(Z_1, Z_2)$ is the nuclear stopping power for the ion-target combination Z_1, Z_2; α is a factor depending only on m and M_2/M_1, but for most purposes can be taken to be independent of m; and U_0 is the surface binding energy. Equation 57 therefore suggests that the ratio

$$\frac{S_{z_1 \cdot z_2}}{S_{\text{self}}} = \frac{S_n(Z_1, Z_2)\ .\ \alpha(M_2/M_1)}{S_n(Z_2, Z_2)\ .\ \alpha(1)} \qquad (58)$$

should be independent of surface saturation effects if it is assumed that U_0 remains the same for both projectiles at the moment of change. Andersen and Bay [39] found experimentally that this ratio is insensitive to previous bombardments of the target surface and agrees reasonably well with Sigmund's theory. Fig. 10 shows a plot of this sputtering yield ratio as a function of the atomic number of the incident ion. The smooth curve indicates that the nuclear stopping power in copper exhibits no oscillations as a function of Z_1.

4. Sputtering efficiency

We have seen that sputtering is a typical multiple collision process involving a cascade of moving target atoms. Obviously in the sputtering process, not all the energy of the incoming ion is deposited within the target. Some of it will be contained in sputtered and backscattered particles leaving the surface. Sigmund [10] defines sputtering efficiency, γ, as the fraction of bombarding ion energy leaving a crystal via sputtering and backscattering:

$$\gamma = \frac{E_{\text{out}}}{E_{\text{in}}} \qquad (59)$$

He has calculated this quantity for the case of perpendicular incidence on a random medium with a plane surface and shown that, unlike the sputtering yield, the sputtered energy is much less sensitive to surface conditions as reflected by variations in the surface binding force. Thompson [1] has measured the energy spectrum of polycrystalline gold bombarded by 41 keV Ar^+ ions and 45 keV Xe^+ ions using a time-of-flight technique. His results show that the number of particles ejected from the surface is determined by the dense low-energy part of the spectrum and is therefore very sensitive to the surface binding energy, while the total energy depends much more on the few high energy particles in the spectrum,

which are influenced relatively little by the surface. Sigmund has shown in his calculations of sputtering efficiency, γ, that the effect of surface binding can be neglected as long as the ion energy is over 1 keV. It thus appears that a direct measurement of γ will give possibly even more reliable information in the sputtering phenomenon than, say, measurements of the sputtering yield which have been widely carried out in the past decade.

In his calculations Sigmund makes use of the spatial distribution of energy deposited by ion bombardment determined previously [11]. He defines $f_D(x)\,dx$ as the average energy deposited in a layer of thickness dx at depth x from the starting point. The assumptions made are that: (i) the target medium is random and infinite; (ii) the collisions are elastic, and (iii) the scattering cross section is given by that derived by Lindhard *et al* [7, 8] (see Equation 19). Then for the target surface at 0, we have:

$$\gamma = \frac{1}{E}\int_{-\infty}^{0} f_D(x)\,dx\,. \qquad (60)$$

To calculate $f_D(x)$ Sigmund makes use of Edgeworth's expansion in terms of spatial moments over the energy distribution. He puts

$$\frac{1}{E} f_D(x)\,dx \equiv f_D(\xi)\,d\xi \qquad (61)$$

where

$$\xi = (x - \langle x\rangle)/\mu_2^{\frac{1}{2}} \qquad (62)$$

is a dimensionless variable which eliminates the energy dependence, and

$$\mu_n = \langle (x - \langle x\rangle)^n\rangle \quad n = 2, 3, 4 \ldots \qquad (63)$$

$\langle x\rangle$ is given by Equation 32, $f_D(\xi)$ can then be approximated by N terms in Edgeworth's expansion

$$f_D(\xi) \simeq f_N(\xi) = \sum_{n=2}^{N} a_n(\xi)\,. \qquad (64)$$

The expansion on the r.h.s. is convergent.
The sputtering efficiency can now be redefined as:

$$\gamma = \frac{1}{E}\int_{-\infty}^{0} f_D(x)\,dx \equiv \int_{-\infty}^{-\langle x\rangle/\mu_2^{\frac{1}{2}}} f_D(\xi)\,d\xi\,. \qquad (65)$$

Values of γ calculated from Equation 65 show that: (i) γ is essentially independent of ion energy in the range above 1 keV, and (ii) γ depends on the ion-target combination through the mass ratio M_2/M_1. One striking result is that γ tends to increase with decreasing ion mass, though it is known from experiment that sputtering yield tends to show the opposite behaviour.

The only investigation of sputtering efficiency so far has been that by Andersen [40] using a rather complicated calorimetric method. He measured γ for graphite, aluminium, silicon, copper, silver, tantalum and lead with 30 to 75 keV He^+, C^+, Ne^+, Ar^+, Cu^+, Kr^+, Xe^+ and Pb^+ ion at perpendicular incidence, to an accuracy of $\pm$ 15%. The results obtained were in good agreement with Sigmund's theoretical prediction.

Acknowledgement

We would like to thank the National Physical Laboratory for financial support while this work was in progress.

References

1. M. W. THOMPSON, *Phil. Mag.* **18** (1968) 377.
2. P. SIGMUND, *Phys. Rev.* **184** (1969) 383.
3. W. BRANDT and R. LAUBERT, *Nucl. Instr. Meth.* **47** (1967) 201.
4. J. B. SANDERS, thesis, University of Leiden (1967).
5. M. W. THOMPSON, "Defects and Radiation Damage in Metals" (Cambridge University Press, 1969).
6. J. LINDHARD, V. NIELSEN, M. SCHARFF, and P. V. THOMSON, *Kgl. Danske Videnskab Selskab, Mat.-Fys. Medd.* **33** no. 10 (1963).
7. J. LINDHARD, M. SCHARFF, and H. E. SCHIØTT, *ibid* **33** no. 14 (1963).
8. J. LINDHARD, V. NIELSEN, and M. SCHARFF, *ibid* **36** no. 10 (1968).
9. J. B. SANDERS, *Canad. J. Phys.* **46** (1968) 455.
10. P. SIGMUND, *ibid* **46** (1968) 731.
11. P. SIGMUND and J. B. SANDERS, Proc. of Intnl. Conf. on Appl. of Ion Beams to Semicond. Technology (Editions Ophrys, Paris, 1967). p. 215.
12. E. SAWATZKY and E. KAY, *Rev. Sci. Instrum.* **37** (1966), 1324.
13. I. S. T. TSONG, *Phys. Stat. Sol.* (a) **7** (1971) 451.
14. P. CIUTI, *Nucl. Instrum. Meth.* **79** (1970) 55.
15. R. J. MACDONALD, *Phil. Mag.* **21** (1970) 519.
16. D. J. MAZEY, R. S. NELSON, and R. S. BARNES, *ibid* **17** (1968) 1145.
17. M. BADER, F. C. WITTEBORN, and T. W. SNOUSE, NASA Report No. TR-R-105, Washington (1961).
18. O. C. YONTS, C. E. NORMAND, and D. E. HARRISON, *J. Appl. Phys.* **31** (1960) 447.
19. O. ALMEN and G. BRUCE, *Nucl. Instrum. Meth.* **11** (1961) 257.
20. A. L. SOUTHERN, W. R. WILLIS, and M. T. ROBINSON, *J. Appl. Phys.* **34** (1963) 153.
21. P. K. ROL, J. M. FLUIT, and J. KISTEMAKER, *Physica* **26** (1960) 1000.
22. M. I. GUSEVA, *Soviet Phys. Solid State* **1** (1959) 1410.
23. C. H. WEIJSENFELD, *Philips Res. Rep. Supp.* No. 2 (1967).

24. G. DUPP and A. SCHARMANN, *Z. Physik* **192** (1966) 284.
25. G. V. JORGENSEN and G. K. WEHNER, *J. Appl. Phys.* **36** (1965) 2672.
26. P. D. DAVIDSE and L. I. MAISSEL, *J. Vac. Sci. Technol.* **4** (1967) 33.
27. C. E. RAMER, M. A. BARASIMHAM, H. K. REYNOLDS and J. C. ALLERD, *J. Appl. Phys.* **35** (1964) 1673.
28. H. BACH, *J. Non-Cryst. Solids* **3** (1970) 1.
29. J. LINDHARD, *Kgl. Danske Videnskab Selskab Mat. Fys. Medd.* **34** no. 14 (1965).
30. I. N. EVDOKIMOV and V. A. MOLCHANOV, *Canad. J. Phys.* **46** (1968) 779.
31. V. A. MOLCHANOV and V. G. TELKOVSKII, *Soviet Phys. Doklady* **6** (1961) 397.
32. G. DUPP and A. SCHARMANN, *Z. Physik* **194** (1966) 448.
33. K. B. CHENEY, and E. T. PITKIN, *J. Appl. Phys.* **36** (1965) 3542.
34. A. J. SUMMERS, J. J. FREEMAN, and N. R. DALY, *J. Appl. Phys.* **42** (1971) 4774.
35. H. BACH, *Naturwissenschaften* **55** (1968) 439.
36. G. K. WEHNER, R. V. STUART, and D. ROSENBERG, General Mills Annual Report of Sputtering Yields, Report No. 2243 (1961).
37. H. BACH, *Nucl. Instrum. Meth.* **84** (1970) 4.
38. *Idem, Z. Naturforsch.* **27a** (1972) 333.
39. H. H. ANDERSEN and H. BAY, *Radiation Effects* **13** (1972) 67.
40. H. H. ANDERSEN, *ibid* **3** (1970) 51.

Received 5 May and accepted 22 May 1972.